Dalton Transactions

ROYAL SOCIETY OF CHEMISTRY

PAPER

View Article Online
View Journal | View Issue

Check for updates

Cite this: *Dalton Trans.*, 2023, **52**, 3835

Polarized Au(I)/Rh(I) bimetallic pairs cooperatively trigger ligand non-innocence and bond activation†

Macarena G. Alférez, Juan J. Moreno, Celia Maya and Jesús Campos *

Received 8th February 2023,
Accepted 21st February 2023

DOI: 10.1039/d3dt00410d

rsc.li/dalton

The combination of molecular metallic fragments of contrasting Lewis character offers many possibilities for cooperative bond activation and for the disclosure of unusual reactivity. Here we provide a systematic investigation on the partnership of Lewis basic Rh(I) compounds of type $[(\eta^5\text{-L})Rh(PR_3)_2]$ (η^5-L = $(C_5Me_5)^-$ or $(C_9H_7)^-$) with highly congested Lewis acidic Au(I) species. For the cyclopentadienyl Rh(I) compounds, we demonstrate the non-innocent role of the typically robust $(C_5Me_5)^-$ ligand through migration of a hydride to the Rh site and provide evidence for the direct implication of the gold fragment in this unusual bimetallic ligand activation event. This process competes with the formation of dinuclear Lewis adducts defined by a dative Rh → Au bond, with selectivity being under kinetic control and tunable by modifying the stereoelectronic and chelating properties of the phosphine ligands bound to the two metals. We provide a thorough computational study on the unusual Cp* non-innocent behavior and the divergent bimetallic pathways observed. The cooperative FLP-type reactivity of all bimetallic pairs has been investigated and computationally examined for the case of N–H bond activation in ammonia.

Introduction

The area of bimetallic cooperativity has witnessed a rapid resurgence in the last decades, in great part due to the prospects it offers for bond activation and catalysis.[1] The same can be stated about heterogeneous[2] and enzymatic catalysis,[3] where bi- and multimetallic synergisms are at the heart of many successful chemical transformations. Beyond catalytic applications, molecular dinuclear structures offer a range of possibilities that have led to the observation of remarkable electronic, magnetic or photophysical properties, exotic bonding schemes and highly unusual reactivity, including an outstanding capacity to trap otherwise fleeting species.[1] For instance, our group recently unlocked a new mode of ligand non-innocent behavior discernible only through a bimetallic approach. More precisely, we described the direct involvement of the widespread pentamethyl cyclopentadienyl ($[C_5Me_5]^-$, Cp*) ligand, whose popularity largely relies on its assumed robust spectator character, in the migration of a hydride from one of its methyl groups in compound $[(\eta^5\text{-}C_5Me_5)Rh(PMe_3)_2]$ (**1a**) to the rhodium centre (Fig. 1),[4] a process which was so far restricted to early transition metals.[5] As introduced above, we were capable of characterizing this reversible event leveraging a bimetallic approach, more precisely by introducing the highly electrophilic and sterically shielded $[(PCyp_2Ar^{Xyl2})Au]^+$ fragment[6] (Cyp = cyclopentyl; Ar^{Xyl2} = C_6H_3-2,6-(C_6H_3-2′,6′-Me_2)$_2$).

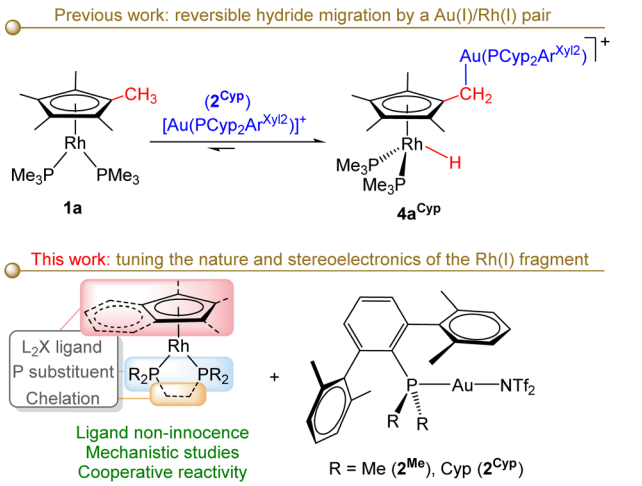

Fig. 1 Cp* non-innocence by reversible hydride migration in a Rh(I)/Au(I) system and systematic investigation carried out in this work on the effects of tuning the Rh(I) fragment.

Instituto de Investigaciones Químicas (IIQ), Departamento de Química Inorgánica and Centro de Innovación en Química Avanzada (ORFEO-CINQA), Consejo Superior de Investigaciones Científicas (CSIC) and University of Sevilla, Avenida Américo Vespucio 49, 41092 Sevilla, Spain. E-mail: jesus.campos@iiq.csic.es; https://jcam-posgroup.iiq.us-csic.es/

†Electronic supplementary information (ESI) available: Experimental procedures, NMR studies and computational details. CCDC 2223979–2223987. For ESI and crystallographic data in CIF or other electronic format see DOI: https://doi.org/10.1039/d3dt00410d

We could conclude that hydride migration from Cp* occurs in a reversible manner, suggesting that there is potential to design proton-coupled-electron-transfer (PCET) catalysis based on this approach.[7] In fact, this has already been demonstrated for hydrogen evolution and dinitrogen reduction by means of a related reversible proton migration between late transition metals and the internal carbon atoms of Cp ligands.[8] However, before embarking ourselves into similar endeavors based on the methyl functionalities of Cp*, it is necessary to better understand the factors influencing the described non-innocence, as well as the precise role associated to the gold moiety. Besides, in terms of intermolecular reactivity, the aforesaid Rh(I)/Au(I) pairs render potential for bimetallic bond activation processes. Thus, as highly constrained metallic fragments of opposed Lewis character, they may behave as bimetallic frustrated Lewis pairs (FLPs),[9] a nascent topic to which we have contributed in recent years.[10] Nonetheless, the Cp* non-innocence described herein advises for the exploration of alternative aromatic capping ligands in our continuous search for bimetallic FLPs.

In this context, we have decided to modify the Lewis basic Rh(I) precursor $[(\eta^5\text{-}C_5Me_5)Rh(PMe_3)_2]$ (**1a**) to investigate the effects on ligand non-innocence and bimetallic Rh(I)/Au(I) reactivity. To do so we have tuned the stereoelectronic and chelating properties of the phosphine ligands and the outcomes resulting from substituting the Cp* fragment by the also prevalent indenyl ($[C_9H_7]^-$) ligand, which lacks $C(sp^3)$–H groups (Fig. 1). We provide a thorough computational investigation to ascertain the mechanism by which the hydride reversibly exchanges positions between Cp* and rhodium and for the cooperative bimetallic activation of polar N–H bonds in ammonia.

Results and discussion

We first decided to examine the effects of modifying the simple trimethyl phosphine ligands in **1a**. To circumvent the possibility of ligand dissociation during Cp* and small molecule activation, we selected the chelating bisphoshpines 1,2-bis(dimethylphosphino)ethane (dmpe) and 1,2-bis(diphenylphosphino)ethane (dppe), which led to compounds **1b** and **1c**, respectively (see Scheme 1). These compounds were prepared following the same procedure employed to access **1a**, that is, by reducing dimer $[(\eta^5\text{-}C_5Me_5)RhCl_2]_2$ with sodium amalgam in the presence of the corresponding phosphine (see ESI† for details). In terms of the electrophilic gold fragment, we focused on two precursors of equal formula, $[(PR_2Ar^{Xyl2})Au(NTf_2)]$ ($\mathbf{2^{Me}}$, R = Me; $\mathbf{2^{Cyp}}$, R = Cyp; NTf_2 = $[N(SO_2CF_3)_2]^-$), stabilized by bulky terphenyl phosphine ligands. Although these phosphines are comparable in terms of donating properties,[11] their steric profile is markedly different. Thus, $PCyp_2Ar^{Xyl2}$ is considerably bulkier than PMe_2Ar^{Xyl2}, as evidenced by their percentage buried volumes, recently reported for their corresponding dicoordinate gold–ethylene complexes (PMe_2Ar^{Xyl2}, 38.2% *vs.* PMe_2Ar^{Cyp2}, 53.5%).[12]

As we anticipated, the combination of the rhodium precursor **1b** with gold compounds $\mathbf{2^{Me}}$ and $\mathbf{2^{Cyp}}$ led to analogous reactivity to that observed for the Rh(I) species **1a** (Scheme 1a),[4] owing to their similar stereoelectronic properties. Therefore, the smaller $[(PMe_2Ar^{Xyl})Au]^+$ fragment leads to quantitative formation of the corresponding Rh(I) → Au(I) metal-only Lewis pair (MOLP)[13] ($\mathbf{3b^{Me}}$). In contrast, the more sterically congested $[(PCyp_2Ar^{Xyl})Au]^+$ unit triggers the immediate migration of a hydride towards the rhodium centre with formation of a new Au–CH_2 bond in the Cp*-functionalized

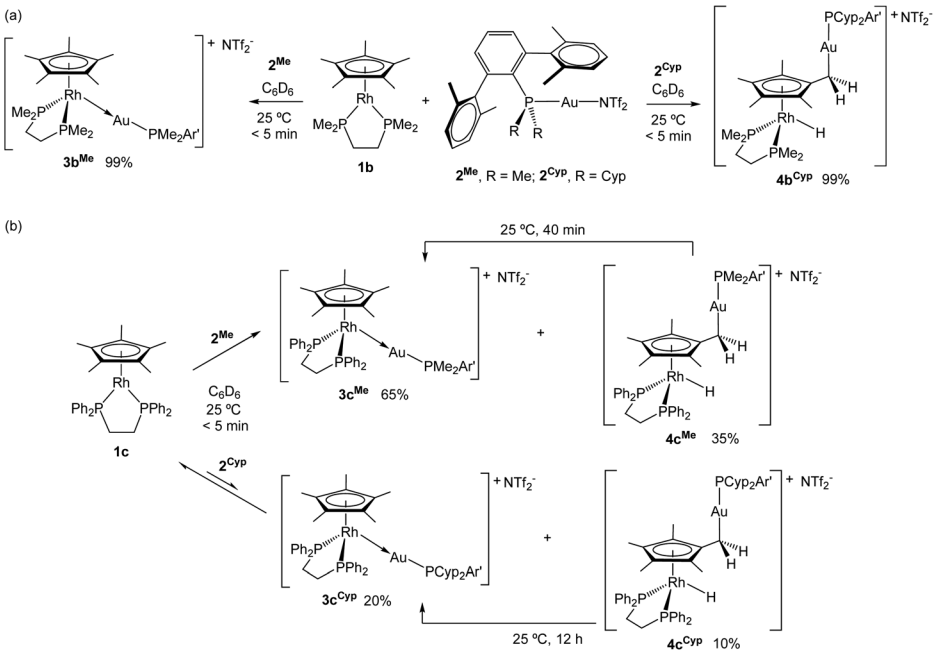

Scheme 1 Contrasting bimetallic reactivity between Lewis basic Rh(I) compounds **1b** and **1c** and Lewis acidic Au(I) compounds $\mathbf{2^{Me}}$ and $\mathbf{2^{Cyp}}$.

compound **4b^{Cyp}**, without any trace of bimetallic dative bonding. The formation of these bimetallic species is easily inferred from multinuclear NMR spectroscopy. A distinctive AB_2 pattern demonstrating the formation of a bimetallic adduct arises in the $^{31}P\{^1H\}$ NMR spectrum of **3b^{Me}**, with an apparent double triplet at 14.6 ppm ($^2J_{PRh}$ = 12, $^3J_{PP}$ = 9 Hz) and a double doublet at 45.5 ppm ($^1J_{PRh}$ = 154, $^3J_{PP}$ = 9 Hz), due to PMe_2Ar^{Xyl2} and dmpe ligands, respectively (*cf.* **3a^{Me}**, 13.9 ppm ($^3J_{PP}$ = 12, $^2J_{PRh}$ = 10 Hz), −3.1 ppm ($^1J_{PRh}$ = 155, $^3J_{PP}$ = 12 Hz)).[4] In turn, the ^1H NMR spectrum of **4b^{Cyp}** reveals the formation of a new hydride ligand resonating at −13.60 ppm (td, $^2J_{HP}$ = 34, $^1J_{HRh}$ = 26 Hz; *cf.* **4a^{Cyp}**, −13.34 ppm, dt, $^2J_{HP}$ = 36, $^1J_{HRh}$ = 25 Hz) and the distinctive asymmetry of the Cp* ligand, now transformed into the $\{C_5Me_4CH_2AuP\}$ moiety, leading to three resonances at 1.74, 1.69 and 1.21 ppm (d, $^3J_{HP}$ = 7.7 Hz) in a 3 : 3 : 1 ratio (*cf.* **4a^{Cyp}**, 1.84, 1.73 and 1.05 ppm ($^3J_{HP}$ = 9.6 Hz)). The molecular structure of **4b^{Cyp}** was authenticated by X-ray diffraction studies from single crystals grown by slow diffusion of pentane into a saturated benzene solution (Fig. 2). Although the overall quality of the crystals was poor, the connectivity was rather clear and certified that the rhodium centre adopts a piano-stool conformation to accommodate the newly form hydride ligand, while the $[(PCyp_2Ar^{Xyl2})Au]^+$ unit displays an orthogonal arrangement relative to the Cp* plane defined by the central five-membered ring (85.22°).

We envisioned that the bulkier and less basic dppe ligand would induce differences in the bimetallic reactivity of precursor **1c** due to steric and electronic effects. In this case, reaction with the smaller PMe_2Ar^{Xyl2}-based gold complex **2^{Me}** not only produced the predicted bimetallic Lewis adduct **3c^{Me}**, but also small amounts of the Cp*-functionalized product **4c^{Me}** in around 30% spectroscopic yield (Scheme 1b). Nonetheless, the latter species rapidly evolves to the thermodynamic product **3c^{Me}**, though its formation suggest that the higher steric pressure exerted by dppe compared to dmpe partially hampers the approximation of the two metal sites and facilitates the detection of **4c^{Me}**, not discernible for neither **1a** nor **1b** for the smaller PMe_2Ar^{Xyl2} gold system. This finding also supports the reversibility of the hydride migration from Cp* to rhodium. Although the isolation of the minor species **4c^{Me}** was not possible, its existence is corroborated by multinuclear NMR analysis. Thus, distinctive resonances in the ^1H NMR are found at −12.30 ppm for the hydride ligand and at 1.99, 1.91 and 0.37 (d, $^3J_{HP}$ = 9 Hz) for the functionalized Cp* ring. $^{31}P\{^1H\}$ NMR resonances recorded at 73.4 ($^1J_{PRh}$ = 139 Hz) and 40.8 ($^2J_{PRh}$ = 9 Hz) ppm due to dppe and PMe_2Ar^{Xyl2} ligands, respectively, are also in agreement with the analogous signals associated to **4a^{Cyp}** and **4b^{Cyp}**.

In stark contrast, when we carried out the same study with the bulkier gold complex **2^{Cyp}** a different scenario ensues: there is virtually no reaction at low temperature (−60 °C). However, upon warming to 25 °C we observe the formation of both the Cp*-activated product **4c^{Cyp}** and the bimetallic Lewis adduct **3c^{Cyp}**, but only as minor species (*ca.* 30% overall), while the monometallic precursors **1c** and **2^{Cyp}** remain as the major components for several hours (Scheme 1b). It is important to remark that despite being the more congested Rh(I) compound, the formation of the bimetallic adduct **3c^{Cyp}** is now preferred over **4c^{Cyp}**, which differs from Rh(I) precursors **1a** and **1b**. We attribute this difference to a shift from kinetic control favouring compounds **4** in the prior systems, to thermodynamic control leading to adducts **3** in the present case, in line with our computational investigations (*vide infra*, Fig. 5). Unexpectedly, the activation product **4c^{Cyp}** is initially formed but it disappears after several hours in favour of a mixture of **1c**, **2^{Cyp}** and **3c^{Cyp}**, evincing the reversibility of the formation of the Au–C bond and concomitant hydride migration, as occurs for the PMe_2Ar^{Xyl2} system. Although we are yet unsure about the reasons on why **4c^{Cyp}** is only discernible initially, it is also true that its overall concentration is variable among different experiments and its initial amount minimal when directly conducting the experiment at 25 °C. In any case, it seems rather clear that **3c^{Cyp}** and **4c^{Cyp}** form from independent reactions from compounds **1c** and **2^{Cyp}**, in agreement with our computational investigations and also with our prior isotopic labelling experiments carried out during ammonia activation studies.

Compounds **1c**, **2^{Cyp}** and **3c^{Cyp}** are in dynamic equilibrium, in line with the reduced basicity of **1c**, which allowed us to spectroscopically investigate the thermodynamics of such a process. A solution of complexes **1c** and **2c^{Cyp}** in benzene-d_6 was monitored for 24 hours to ensure the complete disappearance of **4c^{Cyp}**, then a van't Hoff analysis over a 60 K range yielded thermal parameters for the equilibrium of ΔH = 2.0 ± 0.5 kcal mol^{-1} and ΔS = 8 ± 2 cal K^{-1} mol^{-1}, corresponding to ΔG_{298} = −0.4 ± 1.0 kcal mol^{-1} for the formation of the bimetallic adduct **3c^{Cyp}**. The very small but positive enthal-

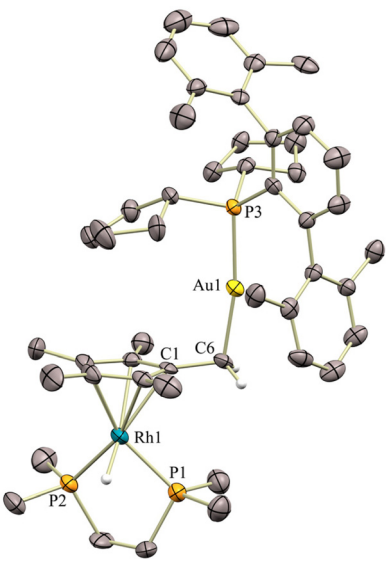

Fig. 2 ORTEP diagram of compound **4b^{Cyp}**; for the sake of clarity most hydrogen atoms, as well as solvent molecules and triflimide counteranions are excluded. Thermal ellipsoids are set at 50% probability.

pic value, along with the only moderately positive entropic component, enable the persistence of variable amounts of the monometallic fragments in solution, a prerequisite for exhibiting bimetallic FLP reactivity.[10]

Therefore, it seems that the higher steric profile of dppe compared to PMe_3 and dmpe, along with the reduced basicity of the rhodium centre, partly impedes the formation of an inactive bimetallic adduct. We tested whether this modulation in bimetallic reactivity has a direct effect on the activation of small molecules, for which we selected the activation of the N–H bond in ammonia. Our choice substantiates on the still challenging character of this activation for transition metal complexes[14] and on our prior finding that **4a^{Cyp}** has already shown success.[4] Compounds **4a^{Cyp}** and **4b^{Cyp}** mediate the heterolytic cleavage of ammonia under mild conditions (1 bar, 25 °C; Scheme 2a), with the former being more rapid ($t_{1/2} \approx$ 30 min), to yield $[(\eta^5\text{-}C_5Me_5)Rh(L_2)H]^+$ (**5a**, L = PMe_3; **5b**, L_2 = dmpe) and $[(PCyp_2Ar^{Xyl2})Au(NH_2)]$.[4] Contrarily, the equilibrium mixture comprised of **1c**, **2^{Cyp}** and **3c^{Cyp}** fails to cleave the N–H bond under similar conditions (Scheme 2b). Instead, only **2^{Cyp}** readily converts into the corresponding ammonia adduct $[(PCyp_2Ar^{Xyl2})Au(NH_3)](NTf_2)$. Subsequently, the mixture slowly evolves to a solution containing the latter adduct and Rh(I) precursor **1c** in detriment of the bimetallic pair **3c^{Cyp}**. Therefore, the reduced basicity of dppe compared to dmpe or PMe_3 hampers the use of the corresponding Lewis basic Rh(I) precursor as a metallic FLP component under these conditions.

Next, we examined the activation of ammonia by computational means. To do so, we decided to focus on the related gold fragment **2^{Tripp}** based on the terphenyl ligand PMe_2Ar^{Tripp2} (Ar^{Tripp2} = C_6H_3-2,6-(C_6H_2-2′,4′,6′-$^iPr_3$)$_2$). We made this choice of ligand to limit the computational difficulties associated to the fluxionality of the cyclopentadienyl groups in $PCyp_2Ar^{Xyl2}$, while at the same time offering similar experimental results to the latter in terms of bimetallic Cp* and ammonia activation.[4] Both metal centers in complex **4a^{Tripp}** are saturated, but the evolution of **4a^{Tripp}** towards the Lewis adduct **3a^{Tripp}** clearly indicates that the independent fragments are accessible in solution (+4.6 kcal mol^{-1} in Fig. 3, **4a^{Tripp}** as reference). Then, the weakly coordinating triflimide in **2^{Tripp}** is readily displaced by ammonia, a reaction that is largely exergonic (9.5 kcal mol^{-1}). Binding to the electrophilic gold(I) center lowers the barrier for deprotonation by the basic Rh center to 15.3 kcal mol^{-1},[15] in a way that is resemblant of conventional FLPs.[16] However, this reaction is thermoneutral relative to the fragments, but overall endergonic relative to **4a^{Tripp}**. We also computed these fragments independently to ensure translational entropy was not responsible for the endergonicity (Fig. 4). We therefore evaluated that, under the reaction conditions, the generated gold amido complex and unreacted **2^{Tripp}** could rapidly evolve to form a bridged amido, cationic digold complex featuring an aurophilic interaction,[4] an event that is more than sufficiently exergonic to drive the reaction forward.

Beyond the mechanism by which cooperative N–H bond activation occurs, we wondered about the precise pathway that accounts for the migration of a hydride from the Cp* ligand to the Rh centre. In our original communication[4] we suggested that an intramolecular migration from a methyl group of the Cp* towards the metal in **1a** would produce a hydride fulvene structure in a process being redox neutral at rhodium, as previously proposed for early transition metals.[5] This highly reactive species could then be trapped by the electrophilic complexes **2**. However, our computational studies indicate that the concerted transition state for the direct transfer of the hydride presented an exceedingly large barrier (TS1 in Fig. 4, 59.7 kcal mol^{-1}) to yield the aforementioned fulvene hydride complex at 21.5 kcal mol^{-1}. Interestingly, Cp* slippage to form an agostic complex presented a much lower barrier (TS2, 31.0 kcal mol^{-1}), from which C–H bond breaking to form the hydride is much more facile (TS3, 25.4 kcal mol^{-1}). Subsequent partial restoration of the Cp* hapticity does not seem rate limiting either (TS4). Nonetheless, these barriers are overly large to be consistent with experimental reaction conditions,[4] which rules out an unassisted intramolecular equilibrium of **1a** to form a fulvene hydride complex. We then sought whether gold complexes **2** could facilitate any of these or other reaction pathways.

Both the Xyl and Tripp systems were computationally studied to gain insight into the role of steric hindrance in the reaction outcome (Fig. 5). Experimentally, we previously observed[4] that while the combination of **1a** and **2^{Xyl}** readily leads to the bimetallic adduct **3a^{Xyl}**, the use of **2^{Tripp}** produces a mixture of **4a^{Tripp}** and **3a^{Tripp}** that eventually evolves towards the later. Thus, the formation of species **4a^{Tripp}** seems to be under kinetic control, as the thermodynamic product is the Lewis adduct. Our computational studies are in agreement with these experimental findings. The Xyl system presents a low barrier (Fig. 5, TS5-Xyl, 11.4 kcal mol^{-1}) for the formation of the Lewis adduct, as expected due to the lower steric demand of the phosphine. In turn, for the Tripp system the transition state lies at 25.3 kcal mol^{-1}, which enables the binding of the gold center to a carbon atom of the anionic Cp* ring (TS6-Tripp, 19.7 kcal mol^{-1}), forming a Rh-diene complex at 5.0 kcal mol^{-1} (**Cp-Au**). This species cannot be accessed by

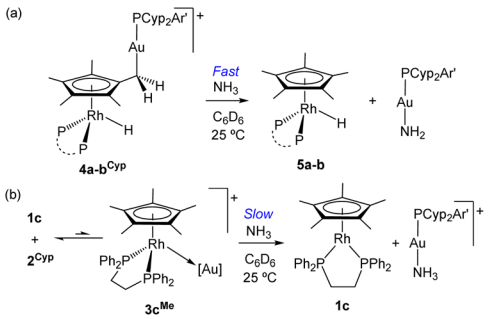

Scheme 2 (a) FLP-type N–H bond activation in ammonia by Rh(I)/Au(I) bimetallic pairs *vs.* (b) no cooperative activation and ammonia adduct formation.

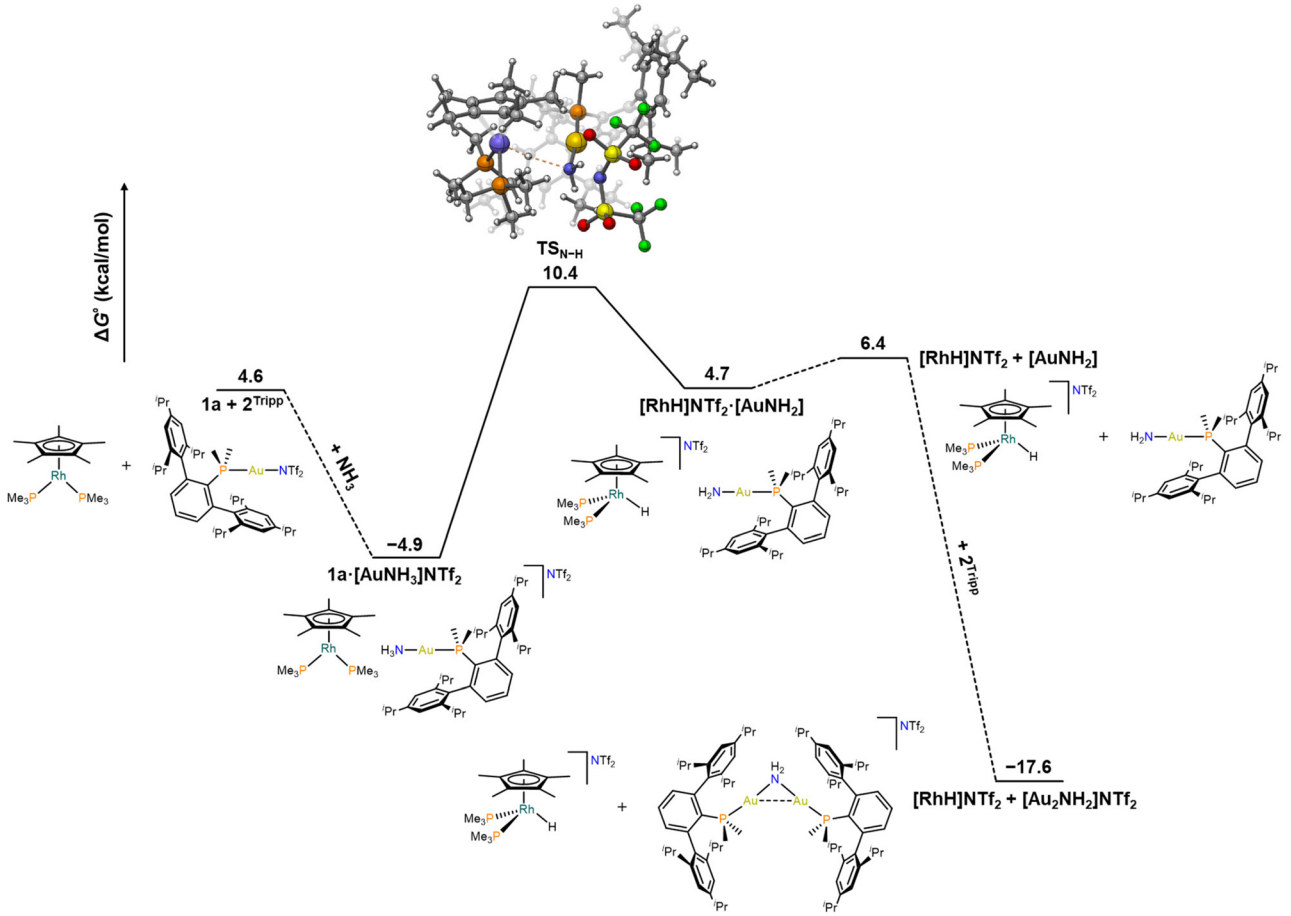

Fig. 3 Free energy profile for the cooperative activation of NH_3, where the zero has been assigned to the Cp*-activated bimetallic compound **4a^{Tripp}**.

the Xyl system, as the barrier for the formation of **3a^{Xyl}** is much lower.

Next, we sought to investigate whether the binding of the electrophilic gold center to the Cp* was indeed key to form **4a^{Tripp}**, that is, to promote hydride transfer to the Rh center concomitant with the formation of the Au–CH_2 bond. Using **Cp-Au^{Xyl}** as a reference, it was clear that despite the pyramidalization that accompanies the formation of the Au–C bond pushing a methyl group towards rhodium, the concerted hydride transfer and gold migration to the nascent CH_2 moiety remains inaccessible (TS7 in Fig. S46,† 49.4 kcal mol^{-1}). In turn, the barrier to form an agostic complex *via* slippage drops to 22.5 kcal mol^{-1} (TS8-Xyl, *cf.* TS2 at 31.0 kcal mol^{-1}), from which hydride formation (TS9-Xyl) lies at 25.0 kcal mol^{-1}, comparable to the unassisted pathway (TS3 in Fig. 4).

We then moved to study the bulkier Tripp system, to ascertain whether these effects were not countered by increased steric demands, as Cp* activation is not observed for the Xyl system. The formation of the corresponding agostic complex for the Tripp system presents a barrier of 25.7 kcal mol^{-1} (TS8-Tripp in Fig. 6), competitive with that of the formation of the Lewis adduct (TS5-Tripp in Fig. 5, 25.3 kcal mol^{-1}), and thus consistent with the aforesaid generation of a mixture of **3a^{Tripp}** and **4a^{Tripp}**. Subsequent steps for the formation of the Rh hydride and for the migration of the gold center towards the CH_2 moiety present similar barriers of 25.7 and 25.4 kcal mol^{-1}, respectively (TS9-Tripp and TS10), affordable under experimental conditions. Although no saddle points could be found, relaxed potential energy scans indicated that the restoration of the Cp* aromaticity to yield **4a^{Tripp}** from **AuCH$_2$** *slipped* was accessible. To complete our computational screening, two alternative pathways, involving hydride abstraction by the Lewis acid and concerted Au–C bond formation concomitant with $HNTf_2$ release were found to be higher energy and are briefly discussed in the ESI (Fig. S47 and S48†).

Therefore, the mechanism for the unusual Cp* non-innocent behavior described herein encompasses the initial binding of the Lewis acidic gold fragment to the Cp* inner ring, which facilitates the migration of the hydride to the rhodium centre by a series of conformational rearrangements that involve the direct participation of both Cp* and gold. These results may have implications in a variety of transformations that imply the use of Cp*-based complexes in the presence of electrophiles. The simplest electrophile would natu-

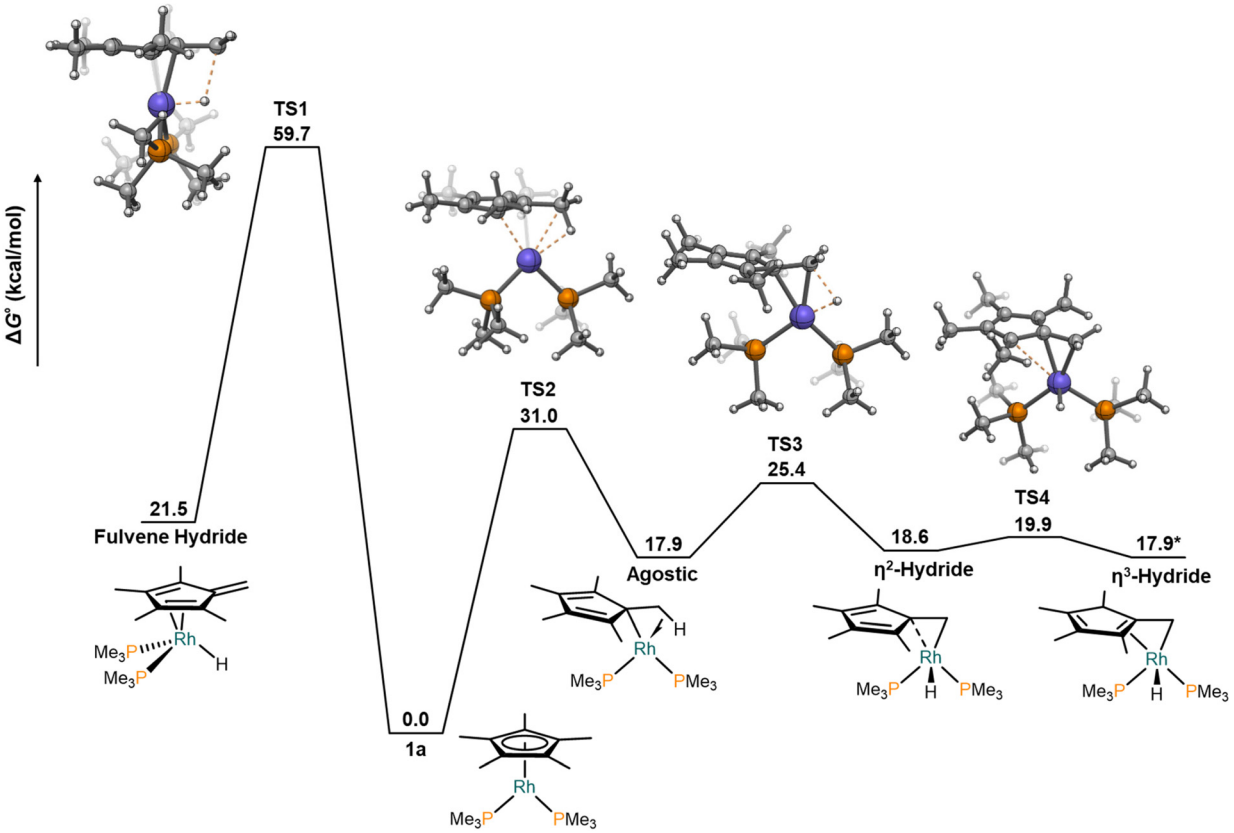

Fig. 4 Free energy profile for the intramolecular conversion of **1a** into a fulvene hydride complex. *SCF energy relative to TS4.

rally be a proton, for which the already discussed protonation of the inner Cp* ring prevails.[8] However, the use of more elaborated electrophiles as additives or co-catalysts in a range of catalytic transformations mediated by Cp*-based complexes is in continuous development.[17] It would not be surprising that the same kind of Cp* non-innocence triggered by the electrophile might be operating in some of these systems, but it could have been overlooked due to difficulties for its identification associated to reversibility and low catalyst loadings. In addition, our studies highlight the importance of controlling the bulkiness of the electrophile (*i.e.* gold fragment), whose subtle tuning dictates selectivity between Lewis adduct formation *vs.* Cp* activation.

With the aim of circumventing the discussed non-innocence character of Cp* to access a broader family of Rh(I)/Au(I) bimetallic FLPs we decided to study analogous Rh(I) precursors based on the well-known indenyl ligand ($[C_9H_7]^-$).[18] Besides, we postulated that the greater capacity of the latter ligand to navigate through variable hapticities (from η^1 to η^5) might offer a richer reactivity after FLP-type bimetallic bond activation. Initially, we prepared the previously reported compound $[(\eta^5\text{-}C_9H_7)Rh(PMe_3)_2]$[19] (**6a**) as our benchmark indenyl-based species. To carry out comparative studies we synthesized analogous Rh(I) species bearing both dppe (**6c**) and the non-chelating and more sterically demanding PPh_3 (**6d**) (see ESI† for synthetic protocols, spectroscopic characterization and X-ray diffraction studies of **6c**), though we omitted a related dmpe version, anticipating identical behavior to **6a** in line to the previously discussed results.

Not surprisingly, the equimolar reaction of **6a** and the smaller gold precursor $\mathbf{2^{Me}}$ led to the corresponding bimetallic adduct $\mathbf{7a^{Me}}$ (Scheme 3a). In this case, the reaction with the bulkier $\mathbf{2^{Cyp}}$ similarly yielded the metal–metal bonded adduct $\mathbf{7a^{Cyp}}$, a behavior attributed to the reduced steric pressure exerted by the indenyl ligand compared to Cp*. The two new adducts exhibit a similar pattern in their $^{31}P\{^1H\}$ NMR spectra, with two doublets due to PMe_3 ($\mathbf{7a^{Me}}$, δ −3.9, $^1J_{PRh}$ = 158 Hz; $\mathbf{7a^{Cyp}}$, δ −6.2, $^1J_{PRh}$ = 159 Hz) and the terphenyl phosphine ($\mathbf{7a^{Me}}$, δ 4.6, $^2J_{PRh}$ = 18 Hz; $\mathbf{7a^{Cyp}}$, δ 43.4, $^2J_{PRh}$ = 19 Hz). At variance with bimetallic adduct $\mathbf{3a^{Me}}$, there is no observable scalar coupling between the two distinct phosphines, a feature attributable to the slightly different geometric environment around rhodium, as evidenced by X-ray diffraction studies (Fig. 7). For instance, the Rh–Au–P angles in the indenyl systems are wider ($\mathbf{7a^{Me}}$, 171.61(7); $\mathbf{7a^{Cyp}}$, 168.21(10)°) than for the Cp* complex $\mathbf{3a^{Tripp}}$ (157.90(11)°), while the greater coordination flexibility of indenyl reflects into wider offset angles between the rhodium centre and the centroid of the η^5-coordinated ring ($\mathbf{3a^{Tripp}}$, 1.85°; $\mathbf{7a^{Me}}$, 10.88°; $\mathbf{7a^{Cyp}}$, 12.35°). Nonetheless, the three structures exhibit comparable Rh–Au bond distances of 2.593(1) ($\mathbf{3a^{Tripp}}$), 2.5541(8) ($\mathbf{7a^{Me}}$) and 2.5970(12) ($\mathbf{7a^{Cyp}}$) Å, in all cases slightly lower than the sum of

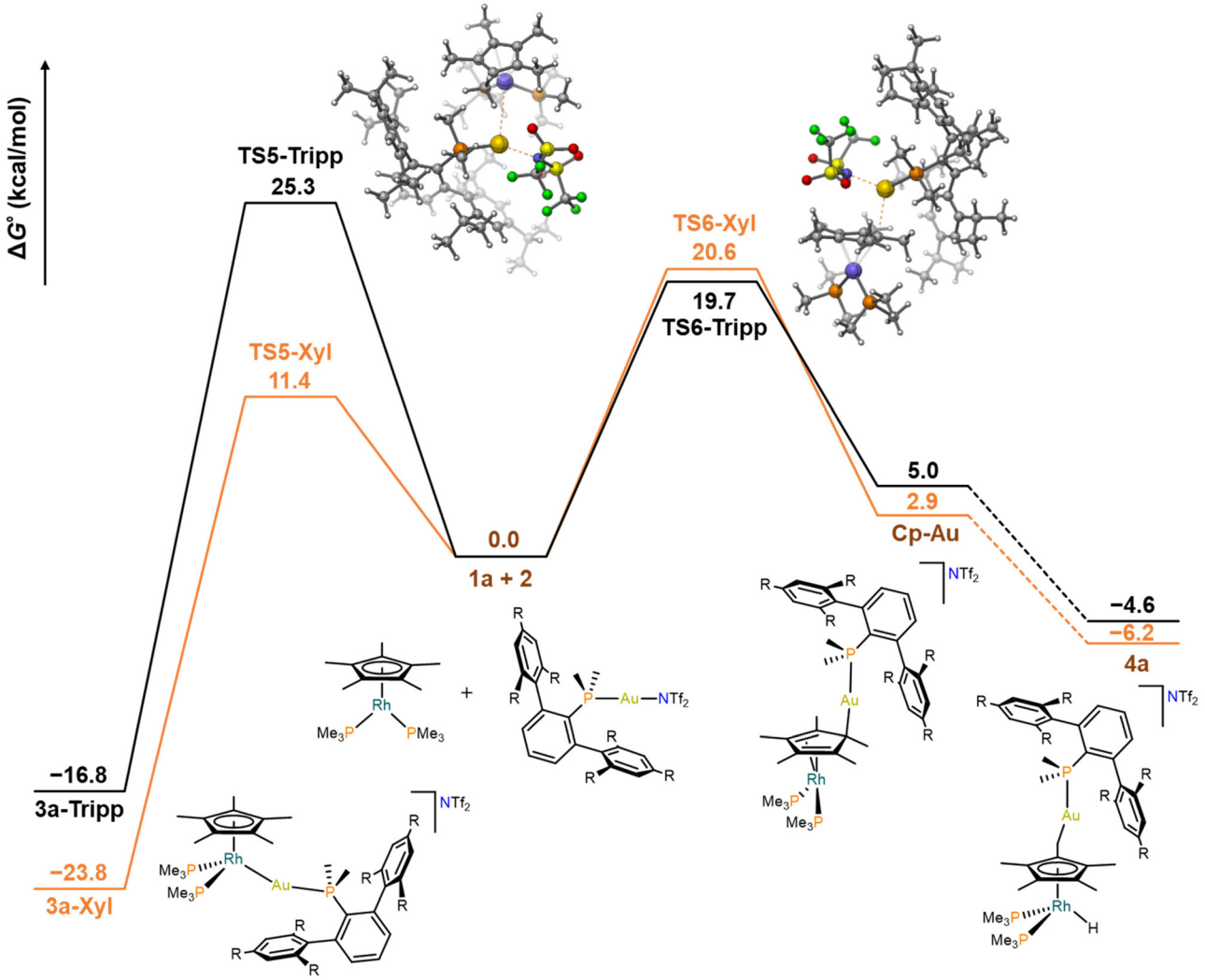

Fig. 5 Free energy profile encompassing Lewis adduct formation, binding of Au(I) to the Cp* and thermodynamics of formation of $\mathbf{4a^{Xyl}}$ (orange) and $\mathbf{4a^{Tripp}}$ (black).

their covalent radii (2.78 Å).[20] Analogously, the calculated formal shortness ratio (FSR),[21] namely the ratio between the M–M bond distance and the sum of their metallic radii, are almost identical and accounts for 1.00 ($\mathbf{3a^{Tripp}}$), 0.99 ($\mathbf{7a^{Me}}$) and 1.00 ($\mathbf{7a^{Cyp}}$).

We then examined the combination of the more congested Rh(I) precursor **6c** with the bulkier Au(I) complex $\mathbf{2^{Cyp}}$. Despite increasing the steric pressure, this mixture cleanly evolves to the corresponding metallic Lewis pair $\mathbf{7c^{Cyp}}$ (Scheme 3a), as inferred from two doublets in the $^{31}P\{^1H\}$ NMR spectrum at 74.7 and 47.0 ppm associated to dppe and $PCyp_2Ar^{Xyl2}$, respectively. Crystals suitable for X-ray diffraction studies were grown by slow diffusion of pentane into a saturated benzene solution of $\mathbf{7c^{Cyp}}$. Interestingly, its ORTEP diagram (Fig. S44†) reveals an elongated Rh–Au bond length of 2.6314(10) Å, though still within the sum of the corresponding covalent radii and with an FSR value of 1.02. Moving towards more congested systems, we examined the analogous reaction with the PPh_3-containing rhodium complex **6d**, in which case the formation of the bimetallic adduct does not take place (Scheme 3b). Instead, we observe broad $^{31}P\{^1H\}$ NMR resonances associated to the corresponding monometallic precursors, indicating dynamic behaviour between these species and the bimetallic adduct. When the reaction is monitored at −20 °C in the NMR probe the resonances narrow, as previously observed for other bimetallic FLPs investigated in our group.[10] The reluctance to form a stable Rh → Au dative bond in this case is most likely due to steric reasons. In fact, treating compound **6d** with the smaller gold complex $\mathbf{2^{Me}}$ does yield the corresponding bimetallic pair $\mathbf{7d^{Me}}$, which was fully characterized by spectroscopic means (see ESI† for details). Besides, its molecular formulation was authenticated by X-ray diffraction studies (Fig. 7), demonstrating the presence of a dative Rh → Au bond characterized by a length of 2.5828(3) Å.

We have previously demonstrated the importance of accessing monometallic fragments in highly polarized and unsup-

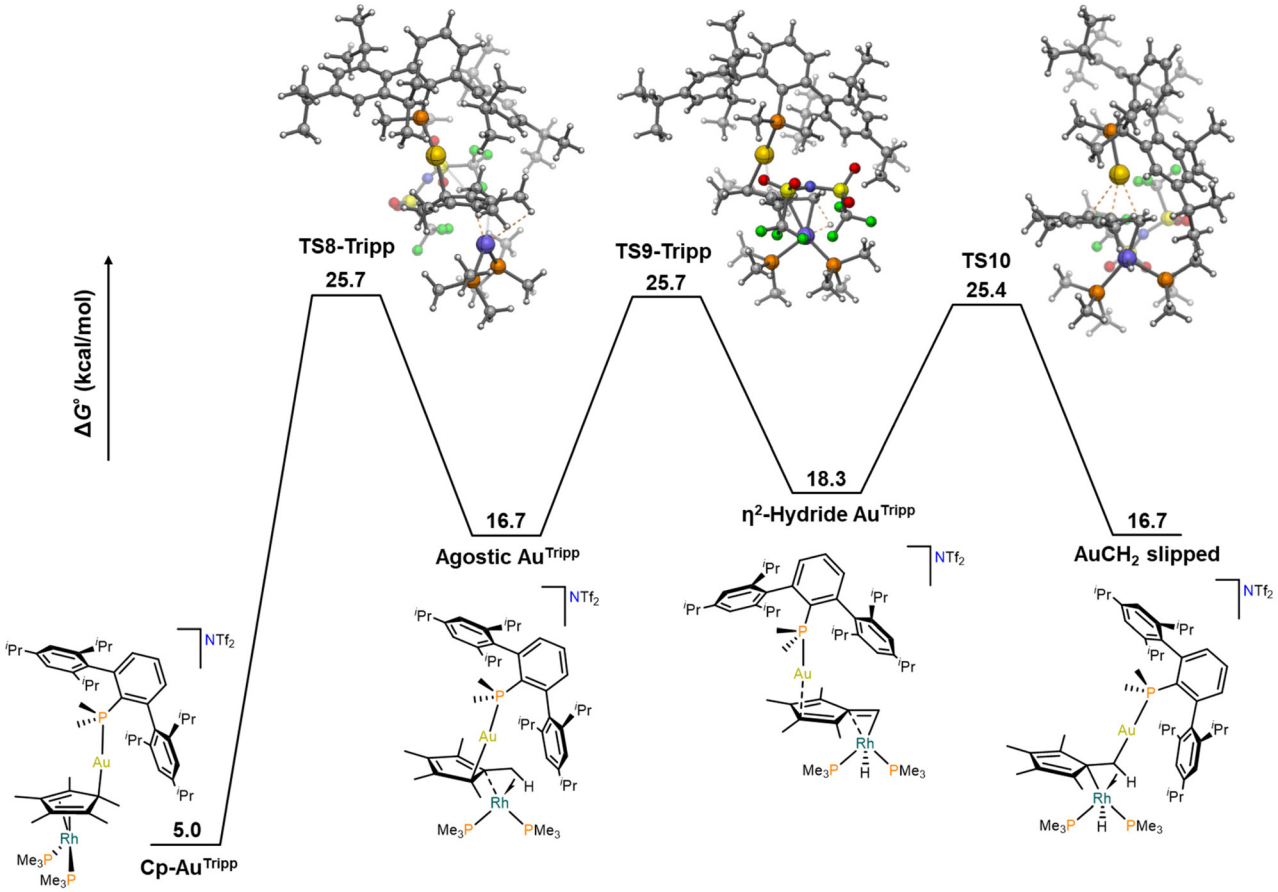

Fig. 6 Free energy profile for the conversion of Cp-Au^{Tripp} into **4a**^{Tripp}.

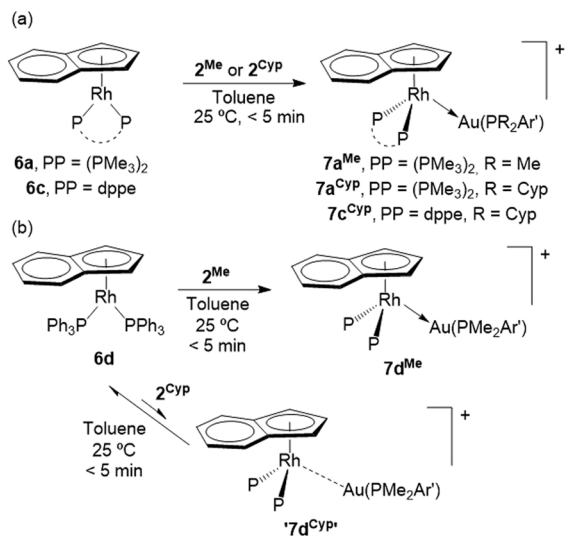

Scheme 3 Bimetallic reactivity between Lewis basic indenyl-Rh(I) compounds **6a**, **6c** and **6d** with Lewis acidic Au(I) compounds **2**^{Me} and **2**^{Cyp}.

ported bimetallic pairs to enhance their cooperative reactivity.[10,22] As such, we promptly explored the reactivity of the non-bonded pair **6d:2**^{Cyp} towards a variety of small molecules containing both non-polar or weakly polarized (H_2, C_2H_2, C_2H_4) and polar bonds (NH_3, H_2O, MeOH). However, instead of the foreseen FLP-type bond activation, we rapidly detected the formation of the heteroleptic gold compound [Au(PCyp$_2$Ar^{Xyl2})(PPh$_3$)] (**8**) (Scheme 4), defined by two distinctive doublets ($^2J_{PP}$ = 309 Hz) at 59.4 and 44.3 ppm by $^{31}P\{^1H\}$ NMR spectroscopy. To assure its formulation this compound was independently prepared and its full characterization is included in the ESI.† Compound **8** is the major and, in some cases, the only discernible gold species obtained during our reactivity studies. Interestingly, the lability of PPh_3 is only evidenced upon addition of small molecules, but it also requires the presence of the gold precursor, since no phosphine dissociation was observed in the absence of **2**^{Cyp}. Further proof of phosphine lability was obtained after attempts to activate ethylene, which led among other species to the presumable formation of [(η^5-C_9H_7)(PPh_3)(C_2H_4)Rh → Au(PCyp$_2$Ar^{Xyl2})](NTf$_2$), inferred from mass spectrometry analysis (see ESI†). Herein, we postulate that substitution of PPh_3 by the smaller ethylene ligand likely facilitates the formation of the dative Rh → Au bond. Likewise, initial efforts to activate isonitriles in an FLP-like manner (*i.e.* 1,1- or 1,2-addition) led to similar results. As an example, addition of 2,6-dimethylphenylisocyanide to a solution of **6d:2**^{Cyp} led to a

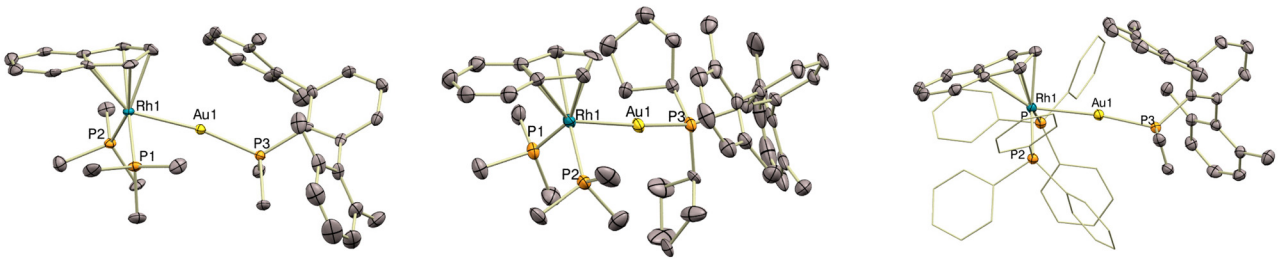

Fig. 7 ORTEP diagrams of indenyl compounds **7a^{Me}**, **7a^{Cyp}** and **7d^{Me}**; for the sake of clarity most hydrogen atoms, as well as solvent molecules and triflimide counteranions are excluded. Some fragments are represented in wireframe format and thermal ellipsoids are set at 50% probability.

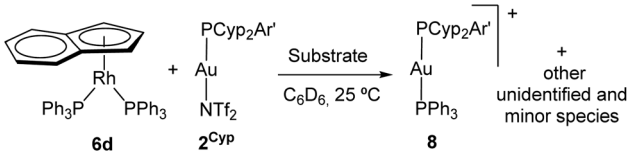

6d **2^{Cyp}** **8**

Scheme 4 Attempts to carry out bimetallic bond activation with a range of substrates (H_2, C_2H_2, C_2H_4, NH_3, H_2O, MeOH and 2,6-dimethylphenylisocyanide) leading to formation of [Au(PCyp$_2$Ar^{Xyl2})(PPh$_3$)].

complex mixture from which a small crop of crystals of [(η^5-C_9H_7(PPh$_3$)(XylNC)Rh → Au(PCyp$_2$Ar^{Xyl2})](NTf$_2$) could be grown and studied by X-ray diffraction (Fig. S44†), once more revealing the lability of PPh$_3$ from Rh(I) and thus limiting its applicability at least in Au(I)-based bimetallic FLPs.

We wondered whether the superior kinetic stability of the chelating dppe ligand would circumvent this drawback while still facilitating the prevalence of the monometallic fragments (bearing in mind the aforesaid elongated Rh → Au bond). However, analogous experiments based on precursor **6b** led to identical results, since the major gold-containing species in all our studies was digold compound [{(PCyp$_2$Ar^{Xyl2})Au}$_2$(μ-dppe)](NTf$_2$)$_2$, characterized by ^{31}P{^{1}H} NMR resonances at 74.9 and 46.5 ppm ($^2J_{PP}$ = 164 Hz) and whose X-ray diffraction structure is provided as well in the ESI (Fig. S44†). We attribute, at least in part, the unexpected facility by which phosphines dissociate in the presence of gold to the weakening of the Rh–P bonds upon the approach of electrophiles. We have computed in recent studies that the strength of the dative bonding between Rh in compound **1a** and a range of metallic electrophiles correlates with greater contributions of $\sigma_{(Rh-P)}$ orbitals, thus weakening Rh–P bonds.[23]

Conclusions

In summary, we provide a systematic study on a series of Rh(I)/Au(I) bimetallic pairs under sterically congested environments. This study evidences the potential for bimetallic cooperation and contrasting reactivity of two metals together compared to their individual mononuclear species. The nature of phosphine ligands bound to either Rh(I) or Au(I) precursors is crucial to control selectivity, where the dominance of either kinetic or thermodynamic products can be precisely tuned. Thus, in the case of [(η^5-C_5Me_5)Rh(PR$_3$)$_2$] compounds, a highly unusual Cp* non-innocent behavior has been described upon addition of the bulkier gold species [(PCyp$_2$Ar^{Xyl2})Au(NTf$_2$)], while the less congested [(PMe$_2$Ar^{Xyl2})Au(NTf$_2$)] system leads to the formation of Rh → Au bimetallic adducts. Nonetheless, the basicity of the phosphines bound to Rh also plays an important role, since for the more congested but less basic dppe ligand the Cp*-activated complexes only appear as transient species. In addition, the stereoelectronic properties of the phosphines dictate the equilibria between bimetallic adducts and individual monometallic compounds for the [(η^5-C_9H_7)Rh(PR$_3$)$_2$] precursors. These equilibria are directly associated to the ability of bimetallic pairs to exhibit frustrated Lewis pair (FLP) behavior, which was observed only for the bulkier Cp*-based Rh system. In contrast, the indenyl analogues were unable to mediate FLP-type bond activation due to the lability of the Rh–P bonds in the presence of gold electrophiles.

Our theoretical studies provide insights about the factors that influence the divergent bimetallic pathways described in this work and the cooperative N–H bond activation of ammonia. Importantly, we now rule out the previously suggested involvement of a fulvene structure trapped by electrophilic gold to account for the reported Cp* non-innocence, as invoked for mononuclear systems based on early transition metals. At variance, we favor a genuine bimetallic pathway that implies the initial binding of gold to the inner Cp* ring, which facilitates proton migration to the basic Rh site and exemplify the potential of bimetallic synergisms. It is likely that this unusual cooperative ligand non-innocence operates in catalytic systems that combine Cp*-based complexes with bulky electrophiles, but its reversible nature and low Cp*-catalyst loadings may have prevented its identification in the past.

Author contributions

M. G. A. synthesized and characterized all compounds. J. J. M. carried out computational studies. M. G. A. and C. M. carried out XRD studies. M. G. A., J. J. M. and J. C. wrote the original draft. J. C. supervised the overall project. All authors contributed to review and editing.

Conflicts of interest

There are no conflicts to declare.

Acknowledgements

This work has been supported by the European Research Council (ERC Starting Grant, CoopCat, 756575). We also thank Grant PID2019-110856GA-I00 funded by MCIN/AEI/10.13039/501100011033, Junta de Andalucía (P18-FR-4688) and US/JUNTA/FEDER, UE (US-1380849). J. J. M. thanks Junta de Andalucía for the postdoctoral program "Personal Investigador Doctor" (ref. DOC_00153). The authors gratefully acknowledge the use of CESGA computational facilities.

References

1 L. H. Gade, *Angew. Chem., Int. Ed.*, 2000, **39**, 2658; J. Park and S. Hong, *Chem. Soc. Rev.*, 2012, **41**, 6931; B. G. Cooper, J. W. Napoline and C. M. Thomas, *Catal. Rev.*, 2012, **54**, 1; J. P. Krogman and C. M. Thomas, *Chem. Commun.*, 2014, **50**, 5115; P. Buchwalter, J. Rosé and P. Braunstein, *Chem. Rev.*, 2015, **115**, 28; J. F. Berry and C. M. Thomas, *Dalton Trans.*, 2017, **46**, 5472; J. F. Berry and C. C. Lu, *Inorg. Chem.*, 2017, **56**, 7577; D. R. Pye and N. P. Mankad, *Chem. Sci.*, 2017, **8**, 1705; I. G. Powers and C. Uyeda, *ACS Catal.*, 2017, **7**, 936; R. C. Cammarota, L. J. Clouston and C. C. Lu, *Coord. Chem. Rev.*, 2017, **334**, 100; N. P. Mankad, *Chem. Commun.*, 2018, **54**, 1291; C. M. Farley and C. Uyeda, *Trends Chem.*, 2019, **1**, 497; J. Campos, *Nat. Rev. Chem.*, 2020, **4**, 696; B. Chatterjee, W.-C. Chang, S. Jena and C. Werlé, *ACS Catal.*, 2020, **10**, 14024; K. Koessler and B. Butschke, *Encyclopedia of Inorganic and Bioinorganic Chemistry*, 2021, DOI: 10.1002/9781119951438.eibc2782; A. M. Borys and E. Hevia, *Trends Chem.*, 2021, **3**, 803; G. Sciortino and F. Maseras, *Top. Catal.*, 2022, **65**, 105; M. Navarro, J. J. Moreno, M. Pérez-Jiménez and J. Campos, *Chem. Commun.*, 2022, **58**, 11220.

2 See for example: S. Zhang, L. Nguyen, J.-X. Liang, J. Shan, J. Liu, A. I. Frenkel, A. Patlolla, W. Huang, J. Li and F. Tao, *Nat. Commun.*, 2015, **6**, 7938; T. Chen and V. O. Rodionov, *ACS Catal.*, 2016, **6**, 4025; M. Filez, *Angew. Chem., Int. Ed.*, 2019, **58**, 13220; A. K. Goulas, S. Sreekumar, Y. Song, P. Kharidehal, G. Gunbas, P. J. Dietrich, G. R. Johnson, Y. C. Wang, A. M. Grippo, L. C. Grabow, A. A. Gokhale and F. D. Toste, *J. Am. Chem. Soc.*, 2016, **138**, 6805.

3 P. A. Lindahl, *J. Inorg. Biochem.*, 2012, **106**, 172; J. Clausen and W. Junge, *Nature*, 2004, **430**, 480; S. J. Lee, M. S. McCormick, S. J. Lippard and U.-S. Cho, *Nature*, 2013, **494**, 380.

4 M. G. Alférez, N. Hidalgo, J. J. Moreno and J. Campos, *Angew. Chem., Int. Ed.*, 2020, **59**, 20863.

5 J. E. Bercaw, *J. Am. Chem. Soc.*, 1974, **96**, 5087; C. McDade, J. C. Green and J. E. Bercaw, *Organometallics*, 1982, **1**, 1629; A. R. Bulls, W. P. Schaefer, M. Serfas and J. E. Bercaw, *Organometallics*, 1987, **6**, 1219; F. G. N. Cloke, J. P. Day, J. C. Green, C. P. Morley and A. C. Swain, *J. Chem. Soc., Dalton Trans.*, 1991, 789.

6 N. Hidalgo, J. J. Moreno, M. Pérez-Jiménez, C. Maya, J. López-Serrano and J. Campos, *Chem. – Eur. J.*, 2020, **26**, 5982.

7 T. Yatabe, T. Kishima, H. Nagano, T. Matsumoto, M. Yamasaki, K.-S. Yoon and S. Ogo, *Chem. Lett.*, 2017, **46**, 74.

8 L. M. A. Quintana, S. I. Johnson, S. L. Corona, W. Villatoro, W. A. Goddard III, M. K. Takase, D. G. VanderVelde, J. R. Winkler, H. B. Gray and J. D. Blakemore, *Proc. Natl. Acad. Sci. U. S. A.*, 2016, **113**, 6409; C. L. Pitman, O. N. L. Finster and A. J. M. Miller, *Chem. Commun.*, 2016, **52**, 9105; M. J. Chalkley, T. J. Del Castillo, B. D. Matson, J. P. Roddy and J. C. Peters, *ACS Cent. Sci.*, 2017, **3**, 217; S. Pal, S. Kusumoto and K. Nozaki, *Organometallics*, 2018, **37**, 906; M. J. Chalkley, T. J. Del Castillo, B. D. Matson and J. C. Peters, *J. Am. Chem. Soc.*, 2018, **140**, 6122; M. J. Chalkley, P. H. Oyala and J. C. Peters, *J. Am. Chem. Soc.*, 2019, **141**, 4721.

9 M. G. Alférez, N. Hidalgo and J. Campos, in *Frustrated Lewis Pairs*, ed. C. Slootweg and A. Jupp, Springer, 2020; M. Navarro and J. Campos, in *Adv. Organomet. Chem*, ed. P. J. Pérez, Elsevier, Amsterdam, 2021, ch. 3, vol. 75.

10 J. Campos, *J. Am. Chem. Soc.*, 2017, **139**, 2944; N. Hidalgo, J. J. Moreno, M. Pérez-Jiménez, C. Maya, J. López-Serrano and J. Campos, *Chem. – Eur. J.*, 2020, **26**, 5982; N. Hidalgo, J. J. Moreno, M. Pérez-Jiménez, C. Maya, J. López-Serrano and J. Campos, *Organometallics*, 2020, **39**, 2534; H. Corona, M. Pérez-Jiménez, F. de la Cruz-Martínez, I. Fernández and J. Campos, *Angew. Chem., Int. Ed.*, 2022, **61**, e202207581.

11 J. J. Moreno, M. F. Espada, J. Campos, J. López-Serrano, S. A. Macgregor and E. Carmona, *J. Am. Chem. Soc.*, 2019, **141**, 2205.

12 M. Navarro, M. G. Alférez, M. de Sousa, J. Miranda-Pizarro and J. Campos, *ACS Catal.*, 2022, **12**, 4227.

13 J. Bauer, H. Braunschweig and R. D. Dewhurst, *Chem. Rev.*, 2012, **112**, 4329.

14 Selected examples of ammonia activation by transition metal complexes: (*a*) J. Zhao, A. S. Goldman and J. F. Hartwig, *Science*, 2005, **307**, 1080; (*b*) C. M. Fafard, D. Adhikari, B. M. Foxman, D. J. Mindiola and O. V. Ozerov, *J. Am. Chem. Soc.*, 2007, **129**, 10318; (*c*) E. Morgan, D. F. MacLean, R. McDonald and L. Turculet, *J. Am. Chem. Soc.*, 2009, **131**(40), 14234; (*d*) J. Abbenseth, M. Kinauer, F. W. Heinemann, C. Wertele, B. de Bruin, S. Schneider and M. G. Scheibel, *Inorg. Chem.*, 2015, **54**, 9290; (*e*) C. C. Almquist, N. Removski, T. Rajeshkumar, B. S. Gelfand, L. Maron and W. E. Piers, *Angew. Chem., Int. Ed.*, 2022, **61**, e202203576.

15 M. J. Bezdek, S. Guo and P. J. Chirik, *Science*, 2016, **354**, 730.

16 Selected examples of FLPs involving initial binding of the substrate to the acidic site: M. A. Dureen, C. C. Brown and D. W. Stephan, *Organometallics*, 2010, **29**, 6594; R. Liedtke, R. Fröhlich, G. Kehr and G. Erker, *Organometallics*, 2011,

30, 5222; O. Ekkerta, G. G. Mieraa, T. Wiegand, H. Eckert, B. Schirmer, J. L. Petersen, C. G. Daniliuc, R. Fröhlich, S. Grimme, G. Kehr and G. Erker, *Chem. Sci.*, 2013, **4**, 2657; M. M. Rahman, M. D. Smith and D. V. Peryshkov, *Inorg. Chem.*, 2016, **55**, 5101; N. Aders, L. Keweloh, D. Pleschka, A. Hepp, M. Layh, F. Rogel and W. Uhl, *Organometallics*, 2019, **38**, 2839; I. Bhattacharjee, S. Bhunya and A. Paul, *Inorg. Chem.*, 2020, **59**, 1046; A. Ullah and G. Q. Chen, *Org. Chem. Front.*, 2022, **9**, 4421.

17 See for example: P. A. Deck, C. L. Beswick and T. J. Marks, *J. Am. Chem. Soc.*, 1998, **120**(8), 1772; S. E. Smith, J. M. Sasaki, R. G. Bergman, J. E. Mondloch and R. G. Finke, *J. Am. Chem. Soc.*, 2008, **130**(6), 1839; S. M. Rummelt and A. Fürstner, *Angew. Chem., Int. Ed.*, 2014, **53**, 3626; Q. Lu, S. Vásquez-Céspedes, T. Gensch and F. Glorius, *ACS Catal.*, 2016, **6**, 2352; J. H. Kim, S. Greßies and F. Glorius, *Angew. Chem., Int. Ed.*, 2016, **55**, 5577; D.-A. Roşca, K. Radkowski, L. M. Wolf, M. Wagh, R. Goddard, W. Thiel and A. Fürstner, *J. Am. Chem. Soc.*, 2017, **139**, 2443; F. Zhao, B. Xu, D. Ren, L. Han, Z. Yu and T. Liu, *Organometallics*, 2018, **37**, 1026; R. Yamada, N. Iwasawa and J. Takaya, *Angew. Chem., Int. Ed.*, 2019, **58**, 17251; J. Liu, H. Song, T. Wang, J. Jia, Q.-X. Tong, C.-H. Tung and W. Wang, *J. Am. Chem. Soc.*, 2021, **143**, 409; R. Tanaka, Y. Hirata, M. Kojima, T. Yoshino and S. Matsunaga, *Chem. Commun.*, 2022, **58**, 76.

18 V. B. Kharitonov, D. V. Muratov and D. A. Loginov, *Coord. Chem. Rev.*, 2019, **399**, 213027.

19 D. J. Parks, W. E. Piers and G. P. A. Yap, *Organometallics*, 1998, **17**, 5492.

20 B. Cordero, V. Gómez, A. E. Platero-Prats, M. Revés, J. Echeverría, E. Cremades, F. Barragán and S. Alvarez, *Dalton Trans.*, 2008, 2832.

21 L. Pauling, *J. Am. Chem. Soc.*, 1947, **69**, 542.

22 N. Hidalgo, F. de la Cruz-Martínez, M. T. Martín, M. C. Nicasio and J. Campos, *Chem. Commun.*, 2022, **58**, 9144; N. Hidalgo, C. Romero-Pérez, C. Maya, I. Fernández and J. Campos, *Organometallics*, 2021, **40**, 1113; N. Hidalgo, C. Maya and J. Campos, *Chem. Commun.*, 2019, **55**, 8812.

23 S. Bajo, M. G. Alférez, M. M. Alcaide, J. López-Serrano and J. Campos, *Chem. – Eur. J.*, 2020, **26**, 16833.